

# Momentum transfer theory of ion transport under the influence of resonant charge transfer collisions: the case of argon and neon ions in parent gases

J.V. Jovanović<sup>1,2</sup>, S.B. Vrhovac<sup>1,a</sup>, and Z.Lj. Petrović<sup>1,b</sup>

<sup>1</sup> Institute of Physics, P.O. Box 68, 11080 Zemun, Belgrade, Yugoslavia

<sup>2</sup> Faculty of Mechanical Engineering, 11000 Belgrade, Yugoslavia

Received 16 June 2002 / Received in final form 2nd August 2002

Published online 24 September 2002 – © EDP Sciences, Società Italiana di Fisica, Springer-Verlag 2002

**Abstract.** Transport properties of ion swarms in presence of Resonant Charge Transfer (RCT) collisions are studied using Momentum Transfer Theory (MTT). It was shown that, not surprisingly, RCT collisions may be represented as a special case of elastic scattering. Using the developed MTT we tested a previously available anisotropic set of cross-sections for Ar + Ar<sup>+</sup> collisions by making the comparisons with the available data for the transverse diffusion coefficient. We also developed an anisotropic set of Ne + Ne<sup>+</sup> integral cross-sections based on the available data for mobility, longitudinal and transverse diffusion. Anisotropic sets of cross-sections are needed for Monte Carlo simulations of ion transport and plasma models.

**PACS.** 51.10.+y Kinetic and transport theory of gases – 52.25.Fi Transport properties – 52.20.Hv Atomic, molecular, ion, and heavy-particle collisions

## 1 Introduction

One of the problems often encountered in studies of the transport of swarms of charged particles is the complexity of the collisional operator which necessitates numerical solution in all realistic cases. Here, under swarm we assume an ensemble of non-interacting (*i.e.* the limit of small ionization) charged particles which are transported in an unperturbed buffer gas under the influence of the external electric field. While numerical techniques for solving Boltzmann equation and for simulations have reached an amazing accuracy [1–4] deepest physical insight may be reached when analytical theories are developed. Momentum transfer theory (MTT) has been developed exactly for that purpose. The theory consists of a specific simplification of the Boltzmann equation collision operator and of the specific procedure to determine approximate distribution function. When swarms develop in uniform and constant fields, the theory yields simple analytic solutions that may be surprisingly accurate and thus may provide basis for fast modeling of plasmas that could be sufficiently fast and accurate. At the same time, relaxation in temporal and spatial inhomogeneities may be included in a consistent manner without losing much of the simplicity (in that case ordinary or simple and well defined partial differential equations have to be solved). Application of MTT in plasma modeling is yet to be pursued, but

we expect [5] that it would be a very viable option for fast models of both local and non-local kinetics in plasmas.

MTT was first used to discuss the diffusion of neutral gases and the mobility of ions at very low field strengths where the energy can always be taken to be entirely thermal [6]. MTT has been initially developed for charged particle transport in mixtures of gases having only elastic collisions [7]. The resulting corrections of Blanc's law [8,9] and the relationship between diffusion coefficients and mobility [9] were obtained. Inelastic collisions have been included in the single gas MTT and the corresponding equations for energy, drift velocity and relationship between the mobility and components of the diffusion tensor were developed. MTT has been developed mainly by the efforts of Robson and coworkers [10,11] as an approximate solution to transport equations which gives an opportunity to develop analytic forms of various transport coefficients and their relations. Reactive collisions were included in addition to inelastic and the corresponding effects of attachment, annihilation [10] and ionization [11] on transport coefficients were discussed. MTT has also been applied in crossed electric  $\mathbf{E}$  and magnetic  $\mathbf{B}$  fields for a case of a single gas in conservative [12] and nonconservative [13] systems. Because of its simplicity which however allows reasonable accuracy MTT has become quite popular in discussing the basic physical explanations of transport phenomena.

We have generalized the MTT for the case of reactive particle swarms in mixtures of gases [14]. This theory was applied to study the development of negative

---

<sup>a</sup> e-mail: vrhovac@phy.bg.ac.yu

<sup>b</sup> e-mail: zoran@phy.bg.ac.yu

differential conductivity [14], the higher order transport coefficients [15] and electron transport in crossed electric and magnetic fields [16].

In this paper we shall discuss an application of MTT to the transport of charged particles under the dominant influence of charge transfer collisions. This case is of utmost importance in numerous plasmas and should be treated in order to develop the basis for applying MTT in plasma modeling. A very basic argument could be used to claim that charge transfer collisions may be represented through elastic scattering. However, this should be shown explicitly. In addition Phelps [17] has pointed out how cross-sections that are obtained by simple conversion of the drift velocity data into momentum transfer and furthermore to the charge transfer cross-sections may be misused in modeling of plasmas. In particular the issue of separation of isotropic and anisotropic (including the backward scattering) components of the cross-sections was shown to be critical in different approaches to plasma modeling.

When ions move in their parent gas, an ion and a neutral can interchange roles by the resonant transfer of an electron. This resonant charge exchange converts a collision having a center-of-mass deflection angle of  $\vartheta$  into one of  $\pi - \vartheta$ . Therefore a large number of glancing collisions are transformed into apparent almost head-on collisions. Resonant charge transfer (RCT) affects ion transport properties in different ways at low and at high electric field strengths [18–20]. At low fields the mean energy that the ions acquire from the field is much less than the thermal energy, the velocity distribution deviates only slightly from the isotropic equilibrium Maxwellian distribution [21]. Main effect is to alter the magnitude and energy dependence of the momentum-transfer cross-section  $Q_1$ . As a result,  $Q_1$  is increased and the temperature (and field) dependence of the mobility  $K$  is drastically altered. At high electric fields, an ion loses most of its energy after a charge transfer (CT) collision. As a result the ion velocity distribution function has low energy maximum and has a long high velocity tail in the field direction. Moreover, the effective kinetic energies of ions that are parallel and perpendicular to the electric field differ substantially. Therefore, both the ion velocity distribution function and the diffusion tensor are strongly anisotropic [22].

We have chosen two examples for numerical calculations. First, we would like to point out that the anisotropy of the diffusion tensor may be used as a critical test of the anisotropic cross-sections that should be developed to properly model the kinetics of ion transport in gases and in plasmas. Thus we shall check the cross-section set proposed by Phelps [17] for argon ions in argon. The second example will consist of determination of the anisotropic set of cross-sections for neon ions at low energies based on both drift velocities and components of the diffusion tensor.

As rare gases are common buffer gases in numerous plasma applications the range of situations where such data would be of use is quite wide. We shall mention few. Sputtering discharges rely [23] on high energy transport

of heavy rare gas ions that would be dominated by the charge transfer collisions and may even lead to a considerable component of sputtering due to fast neutral bombardment. RF plasmas used for etching and other technologies in production of integrated circuits commonly involve argon as a buffer gas [24–26] and both ion [27, 28] and fast neutral distributions at the surface of wafer is the critical issue in understanding both the kinetics of etching and of charging [29–31]. Recently it was proposed that the charge transfer together with neutralization on surface may be used to develop *charging free* etching [32, 33]. The results of this paper may also be of interest for modeling of plasma displays [34] and plasma thrusters [35]. Finally the influence of CT collisions on gas breakdown and glow discharges has been recently studied based on well defined and reliable experimental data [36–44] including the studies at very high  $E/n_0$  (here  $E/n_0$  is the ratio of the electric field  $E$  to the neutral gas number density  $n_0$ ) [45–48].

## 2 Balance equations including charge transfer

### 2.1 Charge transfer model

Our discussion is limited to collisions of symmetric (resonant) ion-atom (molecule) systems, such as  $\text{Ar}^+ + \text{Ar}$  and  $\text{Ne}^+ + \text{Ne}$ , when scattered ion is indistinguishable from the incident ion and we are concerned only with the elastic collisions. We assume that charge (electron) can be transferred without any noticeable transfer of momentum. If the motion of the charged particle is followed, this corresponds to elastic scattering where the velocities of the collision partners are interchanged, *i.e.* where the scattering angle is close to  $\pi$ . The corresponding backward ( $\pi$  in center of mass) peaked component of the differential scattering cross-section  $I_b(v_r, \theta)$  is defined as [49]:

$$I_b(v_r, \theta) = \frac{\sigma_b(v_r)}{2\pi} \lim_{\theta_0 \rightarrow \pi} \delta(\cos \theta - \cos \theta_0). \quad (2.1)$$

Phelps [17] has shown that it is necessary to include also the isotropic part of the differential scattering cross-section which is defined as:

$$I_i(v_r, \theta) = \frac{\sigma_i(v_r)}{4\pi}. \quad (2.2)$$

If  $I(v_r, \theta) = I_b(v_r, \theta) + I_i(v_r, \theta)$  denotes the total differential scattering cross-section, then we define the partial cross-sections [6]:

$$Q_l(v_r) = 2\pi \int_0^\pi d\theta \sin \theta (1 - \cos^l \theta) I(v_r, \theta), \quad l = 1, 2, 3, \dots \quad (2.3)$$

According to equations (2.1–2.3) we have momentum transfer cross-section  $Q_1(v_r) = \sigma_i(v_r) + 2\sigma_b(v_r)$ , and viscosity cross-section  $Q_2(v_r) = (2/3)\sigma_i(v_r)$ . Symmetric charge transfer collisions may be treated as a subset of elastic scattering collisions. At high ion energies  $\sigma_b(v_r)$  is identical to the charge transfer cross-section  $\sigma_{\text{CT}}(v_r)$ , but at low energies there is combination of isotropic and backward scattering contributing to  $Q_1(v_r)$  [17].

## 2.2 Summary of relevant equations

Considering ions of number density  $n$  in neutral gas in equilibrium at temperature  $T_0$  and making the assumptions that density gradients are weak, we have the following approximate balance equations for mean velocity  $\langle \mathbf{v} \rangle$  of ions and average energy  $\langle\langle \varepsilon \rangle\rangle$  in the center of mass frame [10, 14]:

$$-n e \mathbf{E} + k_B \hat{T} \frac{\partial n}{\partial \mathbf{r}} = -\frac{1}{2} m n \langle \mathbf{v} \rangle \nu_m(\langle\langle \varepsilon \rangle\rangle), \quad (2.4)$$

$$\langle\langle \varepsilon \rangle\rangle = \frac{1}{2} m_0 \langle \mathbf{v} \rangle^2 + \frac{3}{2} k_B T_0 - \mathbf{Q} \left( \frac{1}{n} \frac{\partial n}{\partial \mathbf{r}} \right) \frac{1}{\nu_m(\langle\langle \varepsilon \rangle\rangle)}. \quad (2.5)$$

Equations (2.4, 2.5) are valid to the first order in the density gradient  $(\partial/\partial \mathbf{r})n$ . In these equations  $m$  and  $m_0$  denote the masses of an ion and neutral molecule respectively,  $k_B$  is Boltzmann's constant, while mean energy in the laboratory frame is

$$\begin{aligned} \varepsilon_L &\equiv \frac{1}{2} m \langle v^2 \rangle = \frac{1}{M_0} \left[ \langle\langle \varepsilon \rangle\rangle - M \frac{3}{2} k_B T_0 \right], \\ M_0 &= \frac{m_0}{m + m_0}, \quad M = \frac{m}{m + m_0}. \end{aligned} \quad (2.6)$$

The ion temperature tensor  $\hat{T}$  appearing on the left side of equation (2.4) is defined by

$$k_B \hat{T} = m \langle (\mathbf{v} - \langle \mathbf{v} \rangle) \otimes (\mathbf{v} - \langle \mathbf{v} \rangle) \rangle, \quad (2.7)$$

where  $\otimes$  indicates a dyadic product of vectors. Also in equation (2.5) vector

$$\mathbf{Q} = \frac{1}{2} \langle (\mathbf{v} - \langle \mathbf{v} \rangle)^2 (\mathbf{v} - \langle \mathbf{v} \rangle) \rangle, \quad (2.8)$$

is the heat flux per ion. In equations (2.4, 2.5) the quantity

$$\nu_m(\langle\langle \varepsilon \rangle\rangle) = n_0 \sqrt{\frac{2 \langle\langle \varepsilon \rangle\rangle}{\mu}} (\sigma_i + 2\sigma_b), \quad (2.9)$$

denotes the total momentum transfer collision frequency, accounting for all scattering channels, both backward and isotropic. The reduced mass is  $\mu = m m_0 / (m + m_0)$ .

Temperature tensor  $\hat{T}$  and heat conductivity vector  $\mathbf{Q}$  can be evaluated from higher order moment equations. Model collision operators can sometimes be used to obtain analytical expressions for the components of temperature tensor  $\hat{T}$  and the vector heat conductivity  $\mathbf{Q}$ . The constant Mean Free Time (MFT) model assumes a cross-section inversely proportional to the relative velocity  $I(v_r, \theta) \propto v_r^{-1}$ . The usefulness of the MFT model derives from the fact that most real ion-molecule potentials are dominated by the polarization force ( $\propto r^{-5}$ ) at large distances, so that for low relative speeds we have  $I(v_r, \theta) \propto v_r^{-1}$ . Hence, in the so-called "polarization limit", *i.e.* for low  $T_0$  and low  $E/n_0$ , an ion swarm may be expected to conform to this model.

In the case of constant MFT where  $\nu_v$  and  $\nu_m$  are constants, the ion temperatures and heat conductivity are given exactly by the expressions [12, 18, 50–52]:

$$\begin{aligned} k_B T_{\parallel} &= k_B T_0 + A_{\parallel} m_0 \omega^2, & k_B T_{\perp} &= k_B T_0 + A_{\perp} m_0 \omega^2, \\ Q &= B m_0 \omega^3, \end{aligned} \quad (2.10)$$

where

$$A_{\parallel} = \frac{2 \frac{m}{m_0} \left( 2 - \frac{\nu_v(\varepsilon)}{\nu_m(\varepsilon)} \right) + \frac{\nu_v(\varepsilon)}{\nu_m(\varepsilon)}}{4 \frac{m}{m_0} + 3 \frac{\nu_v(\varepsilon)}{\nu_m(\varepsilon)}}, \quad A_{\perp} = \frac{\left( 1 + \frac{m}{m_0} \right) \frac{\nu_v(\varepsilon)}{\nu_m(\varepsilon)}}{4 \frac{m}{m_0} + 3 \frac{\nu_v(\varepsilon)}{\nu_m(\varepsilon)}}, \quad (2.11)$$

$$B = \frac{\left( 1 + \frac{m}{m_0} \right)^2 \left( A_{\parallel} + \frac{1}{2} + \frac{3}{2} \frac{m}{m_0} \right)}{1 + 3 \left( \frac{m}{m_0} \right)^2 + 2 \frac{m}{m_0} \frac{\nu_v(\varepsilon)}{\nu_m(\varepsilon)}} - \left( A_{\parallel} + \frac{1}{2} + \frac{1}{2} \frac{m}{m_0} \right), \quad (2.12)$$

and  $\nu_v(\varepsilon) = n_0 (2\varepsilon/\mu)^{1/2} Q_2(\varepsilon)$  is the collision frequency for viscosity. In these expressions,  $\omega$  and  $\varepsilon$  are, respectively, drift velocity and energy in spatially uniform circumstances and are found from solution of the simple equations:

$$e \mathbf{E} = \frac{1}{2} m \omega \nu_m(\varepsilon), \quad (2.13)$$

$$\varepsilon = \frac{1}{2} m_0 \omega^2 + \frac{3}{2} k_B T_0. \quad (2.14)$$

MTT is exact for constant  $\nu_m$  model in the absence of reactions. In more realistic cases, where  $\nu_v$  and  $\nu_m$  are functions of mean energy, equations (2.10) may be only qualitative approximations. Using numerical results from Monte Carlo calculations, Skullerud [18, 51] investigated the accuracy of equations (2.10–2.12) for cases in which the collision frequency was not constant, but  $Q_2/Q_1$  was calculable. He has found that equations (2.10) is generally a very good approximation for  $k T_{\perp}$ , while equations (2.10) is not as effective as a general approximation for  $k T_{\parallel}$ .

Applying a procedure similar to Robson's [12, 52] on equations (2.4, 2.5), we obtain Generalized Einstein Relations (GER):

$$\begin{aligned} D_{\parallel} &= \frac{k_B T_{\parallel}}{e} K \left( 1 + (1 + \Delta) \frac{d \ln K}{d \ln E} \right), \\ D_{\perp} &= \frac{k_B T_{\perp}}{e} K, \quad \Delta = \frac{Q}{2 k_B T_{\parallel} \omega}, \end{aligned} \quad (2.15)$$

where  $K = \omega/E$  is the mobility. The correction factor  $\Delta$  can be evaluated using equations (2.10–2.12).

## 3 Calculations for real cross-sections

Equations (2.13, 2.14) are to be solved for  $\omega$  and  $\varepsilon$  as a function of  $E/n_0$  and  $T_0$ , for a specified model of interaction  $\sigma_b, \sigma_i$ . Transverse  $D_{\perp}$  and longitudinal  $D_{\parallel}$  diffusion coefficients can then be found from GER equation (2.15).

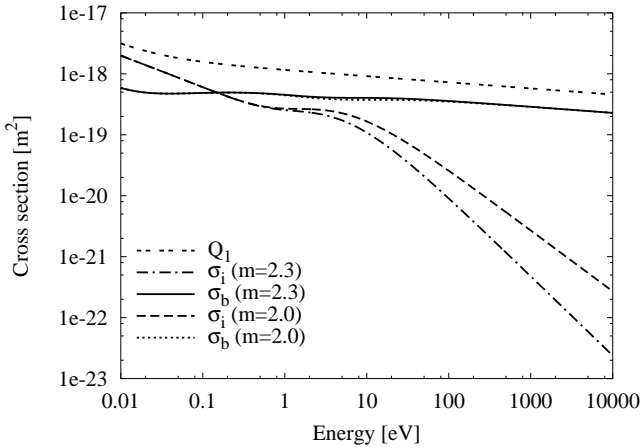


**Fig. 1.** Cross-sections for the elastic scattering of Ar + Ar<sup>+</sup> from reference [17].  $Q_1$ ,  $\sigma_i$  and  $\sigma_b$  are the momentum transfer, isotropic, and backward scattering cross-section components of elastic scattering. Minimum  $\sigma_i$  and maximum  $\sigma_b$  ( $m = 2.3$ ) are shown by the dot-dashed and solid curves, respectively. Suggested values  $\sigma_i$  and  $\sigma_b$  ( $m = 2.0$ ) for plasma modeling, are shown by long-dashed and dotted curves, respectively.

### 3.1 Transport coefficients for Ar<sup>+</sup> in Ar

Recently Phelps [17] has proposed a set of isotropic and backward scattering cross-sections to represent the transport of argon ions in ion buffer gas. The set was primarily based on the available differential cross-section data but also it was tested to fit the available mobilities [45]. It was pointed out that, while small differences exist between the mobilities obtained by standard representations of charge transfer collisions at low energies (either as isotropic scattering by using the momentum transfer cross-section, or by backward scattering only by using CT cross-section) and the model proposed by Phelps, the critical test would consist in calculation of the transverse diffusion coefficient. Recently a set of highly reliable data for transverse diffusion coefficients for argon ions in argon has been obtained [53] that motivated us to perform the tests of the argon scattering model as proposed by Phelps. Earlier studies of the cross-sections for argon ions in their parent gas have been reviewed in [17].

Scattering in this system is described in terms of the consistent sets of Ar<sup>+</sup> + Ar differential and integral cross-sections which were obtained by Phelps from a variety of experimental and theoretical sources. Figure 1 shows various cross-sections defined in Section 2.1 for Ar<sup>+</sup> collisions with Ar. The momentum transfer cross-section  $Q_1$  is known most accurately for a wide range of ion energies. This cross-section is chosen to approach the spiraling cross-section for polarization scattering at low energies [21] and twice the charge transfer cross-section  $\sigma_{CT}$  at high energies [21]. An analytic approximation to the values of the momentum transfer cross-section  $Q_1$  of Figure 1 is [17]:

$$Q_1(\varepsilon) = 1.15 \times 10^{-18} \varepsilon^{-0.1} \left( 1.0 + \frac{0.015}{\varepsilon} \right)^{0.6}. \quad (3.1)$$

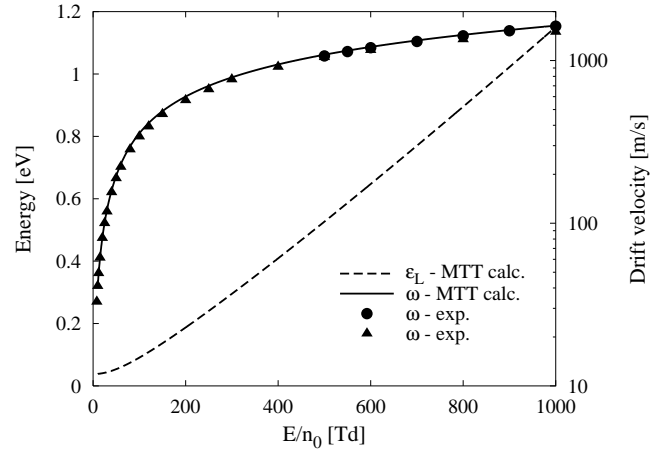


**Fig. 2.** Mean energy  $\varepsilon_L$  and drift velocity  $\omega$  for Ar + Ar<sup>+</sup> as a function of  $E/n_0$ ,  $T_0 = 293$  K. Calculated values are indicated by lines; (●) experimental drift velocities of Hegerberg *et al.* [54]; (▲) experimental drift velocities of Ellis *et al.* [55].

Minimum values of isotropic cross-section  $\sigma_i$  are approximated with the expression [17]:

$$\sigma_i(\varepsilon) = \frac{2.0 \times 10^{-19}}{\varepsilon^{0.5}(1.0 + \varepsilon)} + \frac{3.0 \times 10^{-19} \varepsilon}{(1.0 + \varepsilon/3.0)^m}, \quad (3.2)$$

where  $m = 2.3$ . All the cross-sections are in m<sup>2</sup> and the energies are in eV. The “suggested” (long-dashed curve) cross-section in Figure 1 has been obtained [17] by lowering  $m$  in equation (3.2). Such modification results in a better estimate of the ion scattering at intermediate angles  $\vartheta$ . Values for  $\sigma_b$  are obtained from the  $Q_1$  and  $\sigma_i$  by the relation:

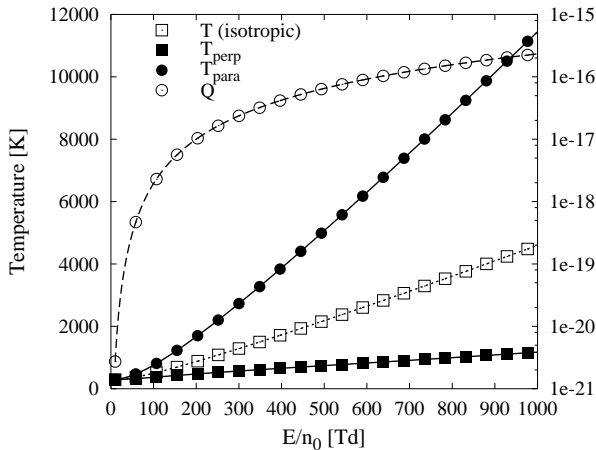
$$\sigma_b(\varepsilon) = \frac{1}{2} (Q_1(\varepsilon) - \sigma_i(\varepsilon)). \quad (3.3)$$

When  $\sigma_i$  is modified it is necessary to change  $\sigma_b$  values by applying this equation.

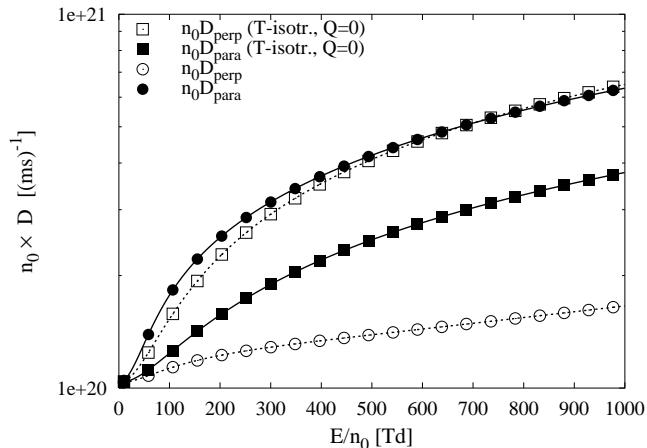
In Figure 2 present mean energy  $\varepsilon_L$  and drift velocity  $\omega$  as a function of reduced field to gas number density ratio  $E/n_0$ , for a standard gas temperature  $T = 293$  K. The points of Figure 2 show measured drift velocities [54, 55], while the solid line shows the values calculated using the momentum transfer cross-section  $Q_1$  of Figure 1 (see Eq. (3.1)) and the MTT equations (2.13, 2.14). MTT calculations yielded results in a very good agreement with the experimental data to within 3% for all values of  $E/n_0$ . The agreement is expected since the cross-section  $Q_1$  in this energy range are those derived from drift velocity data [54] and the minor discrepancy reflects on the accuracy of MTT.

Figure 3 shows the ion temperatures and heat flux as a function of  $E/n_0$ . We have already established that the temperature tensor  $\hat{T}$  is generally anisotropic. Under certain special circumstances temperature tensor can be reduced to a scalar,  $k_B T_{\perp} \approx k_B T_{\parallel} \approx 2\langle\varepsilon\rangle/3$ . For light ions and electrons ( $m \ll m_0$ ) this may be achieved by substituting the condition

$$\frac{m_0 \nu_v}{m \nu_m} \gg 1, \quad (3.4)$$



**Fig. 3.** Isotropic ion temperature  $T$  and the values of temperature coefficients ( $T_{\perp} \equiv T_{\text{perp}}$ ,  $T_{\parallel} \equiv T_{\text{para}}$ ), and heat flux  $Q$  predicted by equations (2.10–2.12) for Ar + Ar<sup>+</sup>, as function of  $E/n_0$ ,  $T_0 = 293$  K.



**Fig. 4.** Diffusion coefficients ( $D_{\perp} \equiv D_{\text{perp}}$ ,  $D_{\parallel} \equiv D_{\text{para}}$ ) for Ar + Ar<sup>+</sup>, as a function of  $E/n_0$ ,  $T_0 = 293$  K; (squares) values obtained for isotropic temperature tensor and  $Q \approx 0$ ; (circles) values obtained using equation (2.15).

in equations (2.10, 2.11). A more general form of the condition (3.4) exists for a more general case which includes inelastic collisions [12]. This condition, however reduces to (3.4) in the case of purely elastic collisions. The isotropy condition (3.4) may not be satisfied for strongly backward scattering, for which  $I(v_r, \vartheta)$  is considerable only for  $\vartheta \approx \pi$ . Then by equation (2.3), we have  $\nu_v \approx 0$  while the momentum transfer collision frequency (2.9) is not necessarily small. This implies anisotropy of the temperature tensor  $\hat{T}$  and breakdown of two term approximation even in the case of light swarm particles [56].

Figure 4 shows diffusion coefficients calculated from GER (Eqs. (2.15)). Since backward scattering dominates over intermediate angle scattering at energies  $\gtrsim 0.2$  eV, *i.e.*  $\sigma_b > \sigma_i$ , the calculated values for the ratio  $D_{\perp}/K$  are very small.

Two comments on ion diffusion coefficients are suggested by Figure 4. First, the dependence of  $D_{\parallel}$  on  $E/n_0$  is much stronger than in the case of  $D_{\perp}$ . This can be at-

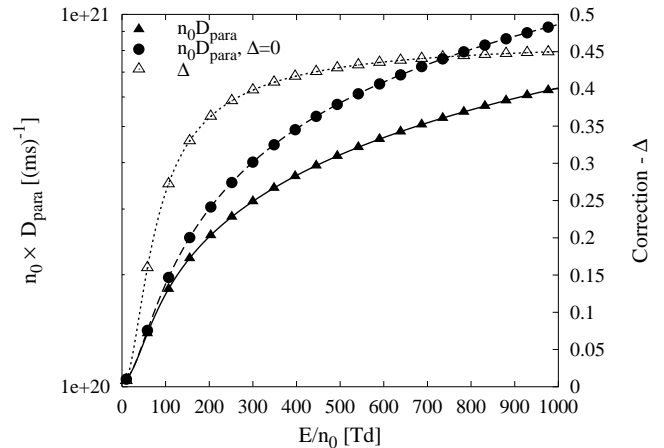


**Fig. 5.** Correction  $\Delta$  predicted by equation (2.15) and longitudinal diffusion coefficient ( $D_{\parallel} \equiv D_{\text{para}}$ ) calculated from GDE (Eq. (2.15)) for Ar + Ar<sup>+</sup>, as a function of  $E/n_0$ ,  $T_0 = 293$  K.

tributed to the different dependencies of  $T_{\parallel}$  and  $T_{\perp}$  on reduced field strength  $E/n_0$ . Figure 3 shows that when  $T_{\parallel}$  is increased by about two orders of magnitude with the  $E/n_0$  increasing from 10 to 1000 Td,  $T_{\perp}$  changes by less than an order of magnitude in the same interval.

The second comment that may be made is that, for higher fields, the assumption of isotropic temperature tensor leads to remarkable differences of the diffusion coefficients, as compared to the calculations based on anisotropic temperature tensor. As expected, the drift velocity is determined by the adopted value of the momentum transfer cross-section  $Q_1$ , and is very little influenced by the angular distribution in the scattering [45]. However, as stressed above, in case of diffusion coefficients the discrepancies are great which indicates the necessity to employ anisotropic models in plasma modeling [17].

The correction factor  $\Delta$  (see Eqs. (2.15)) can be evaluated using equations (2.10–2.12) and its dependence upon  $E/n_0$  for Ar + Ar<sup>+</sup> is shown in Figure 5. The correction  $\Delta$  is of the order of  $10^{-1}$  and approaches zero in the low-field limit. This is a reflection of the similar variation of  $Q$  with  $E/n_0$  (Fig. 3). Figure 5 also shows the comparison of longitudinal diffusion coefficient  $D_{\parallel}$  with the corresponding coefficient, calculated by ignoring the heat transfer ( $Q \approx 0$ ,  $\Delta = 0$ ).

The results of our calculation for the ratio  $D_{\perp}/K$  are shown in Figure 6, where they are compared to the experimental results of Sejkora *et al.* [57], Stefánsson and Skullerud [53] and Schiestl *et al.* [58], respectively. The agreement between calculated and measured values is surprisingly good below 1000 Td, but at higher  $E/n_0$ , the experimental values fall significantly below the calculated ones. Small changes in the isotropic cross-section parameter  $m = 2.0$ – $2.3$  have little influence on this (Fig. 6).

For comparison, we also show (dotted line in Fig. 6) results obtained from a moment theory calculation, which have been carried out by Stefánsson and Skullerud [53], based on an analytical four-parameter model potential. From Figure 6 it is evident that the difference between

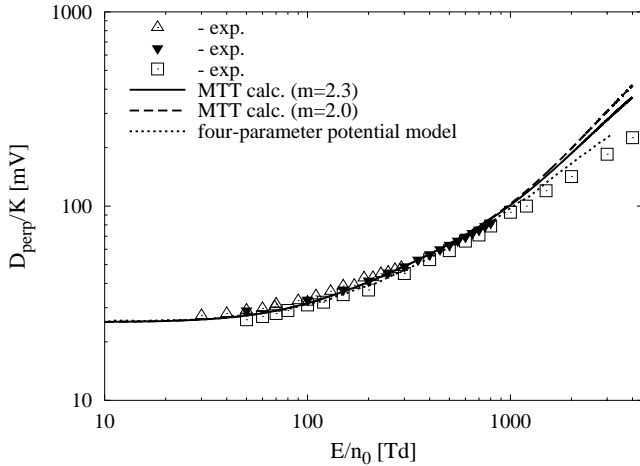


**Fig. 6.** Transverse diffusion coefficient  $D_{\perp} \equiv D_{\text{perp}}$  for  $\text{Ar} + \text{Ar}^+$  as a function of  $E/n_0$ ,  $T_0 = 293$  K; ( $\Delta$ ) experimental values of Sejkora *et al.* [57]; ( $\square$ ) experimental values of Stefánsson and Skullerud [53]; ( $\blacktriangledown$ ) experimental values of Schiestl *et al.* [58].

MTT results and moment theory calculation became important at high-field strengths.

### 3.2 Transport coefficients for $\text{Ne}^+$ in Ne

The available cross-sections in the literature for ion transport at moderately small energies are mostly based on determination of the mobility and subsequent determination of the momentum transfer cross-section. Momentum transfer cross-section was converted to the charge transfer cross-section without any isotropic scattering. The best available data include the mobility measurements of Hegerberg *et al.* [54], Helm and Elford [59], of Skullerud and Larsen [60] and of Basurto *et al.* [61]. The diffusion coefficients or characteristic energies have been measured with high accuracy by Stefánsson [62]. We have performed for neon a similar analysis as Phelps did for argon [17] except that the basis for determining the isotropic part of the cross-section came from the requirement to fit the available experimental data for the transverse component of the diffusion tensor. Of course, the complete set of cross-sections had to agree with all the available transport coefficients in the low energy range (below 2 eV).

At very low energies we allowed the isotropic elastic scattering to aim towards the polarization limit. The complete set of cross-sections is shown in Figure 7. At the higher energy end charge transfer is significantly higher than the isotropic elastic scattering. At even higher energies one could allow the contribution of isotropic component to decrease in a similar way as for argon. We however do not show these data here as the available diffusion coefficient data do not allow exact determination of the cross-section at higher energies. However, one may state that the present cross-sections may be smoothly extrapolated to the high energy limit of the cross-section set compiled and recommended by Phelps [63].

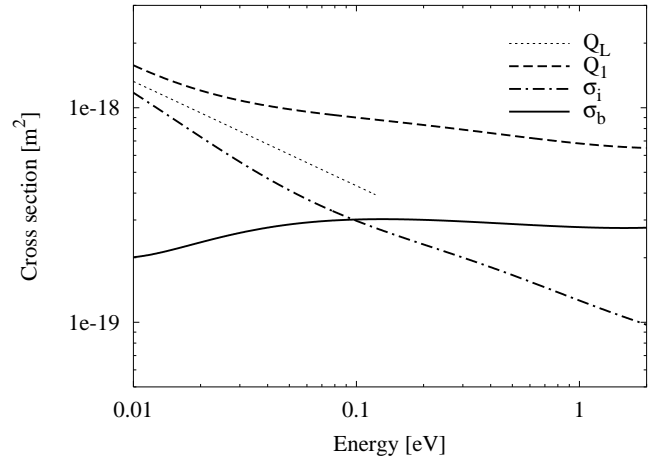


**Fig. 7.** Cross-sections for the elastic scattering of  $\text{Ne} + \text{Ne}^+$ .  $Q_L$ ,  $Q_1$ ,  $\sigma_i$  and  $\sigma_b$  are the polarization spiraling, momentum transfer, isotropic, and backward scattering cross-section components of elastic scattering.

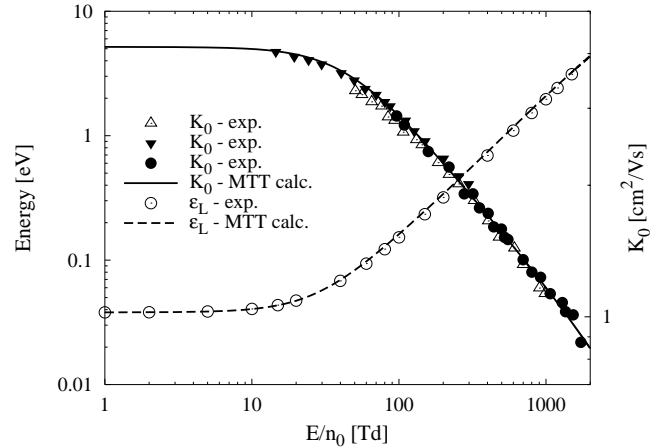


**Fig. 8.** Mean energy  $\epsilon_L$  and reduced mobility  $K_0$  for  $\text{Ne} + \text{Ne}^+$  as a function of  $E/n_0$ ,  $T_0 = 294$  K. Calculated values are indicated by lines; ( $\Delta$ ) experimental reduced mobilities of Hegerberg *et al.* [54]; ( $\blacktriangledown$ ) experimental reduced mobilities of Helm and Elford [59]; ( $\bullet$ ) experimental reduced mobilities of Basurto *et al.* [61]; ( $\circ$ ) calculated mean energies of Skullerud and Larsen [60].

The predictions based on the proposed cross-sections are shown in Figure 8 for the mobility and mean energy, in Figure 9 for the transverse component of the diffusion tensor normalized by the mobility and in Figure 10 for the longitudinal component of the diffusion tensor normalized by the mobility. In all cases agreement is excellent. Having in mind that the cross-section set for argon derived independently gave a very good agreement with the available data one may conclude that the uncertainty due to application of MTT is very small and that the proposed cross-section set is equally reliable.

We should note that it came to our attention that independently of this work Phelps and Pitchford with coworkers have attempted to produce a complete set of cross-sections for the mixture of xenon and neon based on the mobility data of Urquijo *et al.* [64] for mixtures of these

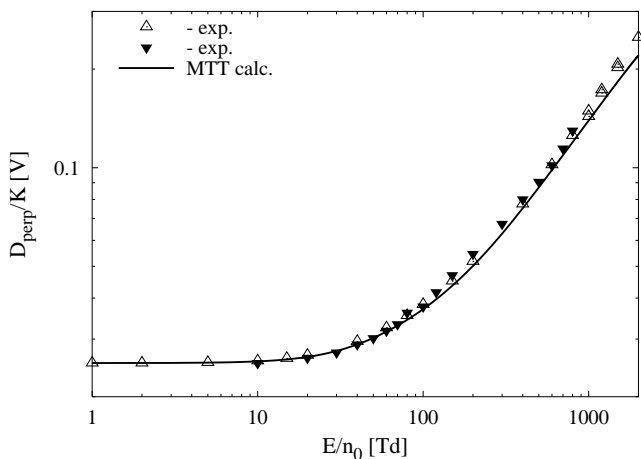


**Fig. 9.** Transverse diffusion coefficient  $D_{\perp} \equiv D_{\text{perp}}$  for  $\text{Ne} + \text{Ne}^+$  as a function of  $E/n_0$ ,  $T_0 = 294$  K; ( $\Delta$ ) experimental values of Skullerud and Larsen [60]; ( $\blacktriangledown$ ) experimental values of Stefánsson [62].

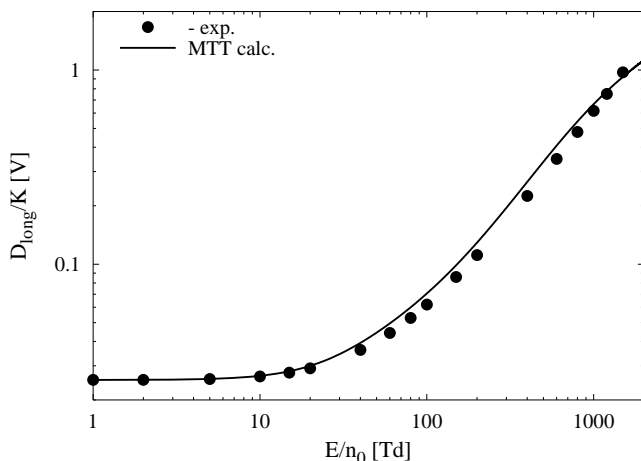


**Fig. 10.** Longitudinal diffusion coefficient  $D_{\parallel} \equiv D_{\text{para}}$  for  $\text{Ne} + \text{Ne}^+$  as a function of  $E/n_0$ ,  $T_0 = 294$  K; ( $\bullet$ ) experimental values of Skullerud and Larsen [60].

two gases. We only had a limited access to some preliminary data up to now so comparisons could not be made.

## 4 Conclusion

The purpose of this paper is to show how transport coefficients under the influence of resonant charge transfer can be approximately treated at high electric fields by momentum-transfer theory [10,14], with particular reference to two issues. The first concerns the choice of consistent ion-atom (molecule) integral cross-sections that take into account differential scattering data and the fact that symmetric charge transfer collisions are one aspect of elastic collisions. The second issue is whether simple MTT calculations in presence of charge transfer collisions give good quantitative estimates of transport coefficients for real gases, such as Ar and Ne.

While one may argue that the applicability of the standard MTT developed for elastic conditions could be ex-

pected, this is by no means a trivial result. One should bear in mind in particular the complex nature of the temperature tensor and of the heat flux vector. Our results show that present semi-quantitative theory fully explains the behavior of the diffusion coefficients with  $E/n_0$  in presence of charge transfer collisions.

Both from the viewpoint of the theory and from the fact that excellent agreement of the results for argon was achieved between experiments and MTT results we may regard the results of MTT as highly reliable. This claim may be extended to all the formulae developed earlier including the GER or Blanc's law (provided that one may be able to define properly the cross-sections for the mixture of gases). The theory may be extended to treat non-resonant (asymmetric) charge transfer and also the transport of the fast atoms produced in the RCT. These components would be required in case that one attempts to develop an MTT based plasma model.

The accuracy of MTT was fully tested for the mobilities and it is certainly not a mere coincidence that the agreement for both components of the diffusion tensor in case of argon is also excellent. At the same time we have verified the anisotropic set of low-energy cross-sections obtained by Phelps [17]. The excellent agreement of the predictions based on the set of Phelps with the experimental data for transverse diffusion give support to both the cross-section set and to the MTT that includes the resonant charge transfer. Having in mind that the transverse diffusion coefficient is particularly sensitive to the isotropic scattering component we were able to propose a set of cross-sections for neon that would satisfy the needs for data for Monte Carlo or kinetic modeling under conditions of plasma sheaths and low pressure-high  $E/n_0$  swarm and discharge experiments.

The simplified model of isotropic plus backward scattering (as proposed by Phelps for argon [17]) provides a good and sufficiently accurate foundation for Monte Carlo simulations and plasma models and may replace the necessity to determine complete differential cross-sections. Experimental data for differential cross-sections for scattering of rare gas ions are not sufficiently detailed and the calculations may involve assumptions of the interaction potentials and complex procedures. Such calculations may yield good results but certainly have to be verified by comparisons with the transport data [65].

Authors are grateful to Dr. R.E. Robson for constant interest, support and useful suggestion. We also wish to acknowledge useful discussions and exchange of information with Dr. A.V. Phelps and Dr. L.C. Pitchford. Authors are also grateful to Saša Dujko for testing some of the results by a Monte Carlo code. Authors wish to acknowledge a very basic support provided by the MNTRS project and an even more substantial support and patience of their families.

## References

1. L.A. Viehland, C.C. Kirkpatrick, *Int. J. Mass Spectrom. Ion Proc.* **149/150**, 555 (1995)
2. T.L. Tan, P.P. Ong, M.J. Hogan, *J. Chem. Phys.* **100**, 586 (1994)

3. T.L. Tan, P.P. Ong, *J. Phys. B* **27**, 1525 (1994)
4. L.A. Viehland, *Chem. Phys.* **179**, 71 (1994)
5. R.E. Robson, R. White, Z.Lj. Petrović, unpublished, 2000
6. E.A. Mason, E.W. McDaniel, *Transport Properties of Ions in Gases* (Wiley-Interscience Publication, New York, 1988)
7. E.A. Mason, H. Hahn, *Phys. Rev. A* **5**, 438 (1972)
8. H.B. Milloy, R.E. Robson, *J. Phys. B: At. Mol. Phys.* **6**, 1139 (1973)
9. J.H. Whealton, E.A. Mason, R.E. Robson, *Phys. Rev. A* **9**, 1017 (1974)
10. R.E. Robson, *J. Chem. Phys.* **85**, 4486 (1986)
11. R.E. Robson, K.F. Ness, *J. Chem. Phys.* **89**, 4815 (1988)
12. R.E. Robson, *Aust. J. Phys.* **47**, 279 (1994)
13. B. Li, R.D. White, R.E. Robson, *Ann. Phys.* **292**, 179 (2001)
14. S.B. Vrhovac, Z.Lj. Petrović, *Phys. Rev. E* **53**, 4012 (1996)
15. S.B. Vrhovac, Z.Lj. Petrović, L.A. Viehland, T.S. Santhanam, *J. Chem. Phys.* **110**, 2423 (1999)
16. Z.Lj. Petrović, S.B. Vrhovac, in *Electron Kinetics and Applications of Glow Discharges*, edited by U. Kortshagen, L.D. Tsendin (Plenum Press, published in cooperation with NATO Scientific Affairs Division, New York and London, 1998), no. 367 in NATO ASI Series, pp. 441–458
17. A.V. Phelps, *J. Appl. Phys.* **76**, 747 (1994)
18. H.R. Skullerud, *J. Phys. B: At. Mol. Phys.* **9**, 535 (1976)
19. S.L. Lin, E.A. Mason, *J. Phys. B: At. Mol. Phys.* **12**, 783 (1979)
20. M. Waldman, E.A. Mason, L.A. Viehland, *Chem. Phys.* **66**, 339 (1982)
21. E.W. McDaniel, E.A. Mason, *The Mobility and Diffusion of Ions in Gases* (John Wiley & Sons, New York, 1974)
22. H.R. Skullerud, *J. Phys. B* **2**, 696 (1969)
23. V.V. Serikov, K. Nanbu, *J. Appl. Phys.* **82**, 5948 (1997)
24. K. Hioki, H. Hirata, S. Matsumura, Z.Lj. Petrović, T. Makabe, *J. Vac. Sci. Technol. A* **18**, 864 (2000)
25. F. Tochikubo, Z.Lj. Petrović, S. Kakuta, N. Nakano, T. Makabe, *Jpn. J. Appl. Phys.* **33**, 4271 (1994)
26. M. Surendra, *Plasma Sources Sci. Technol.* **4**, 58 (1995)
27. J.K. Olthoff, Y. Wang, *J. Vac. Sci. Technol. A* **17**, 1552 (1999)
28. J.K. Olthoff, R.J. VanBrunt, S.B. Radovanov, J.A. Rees, R. Surowiec, *J. Appl. Phys.* **75**, 115 (1994)
29. T.J. Sommerer, M.J. Kushner, *J. Appl. Phys.* **70**, 1240 (1991)
30. K.P. Giapis, T.A. Moore, T.K. Minton, *J. Vac. Sci. Technol. A* **13**, 959 (1995)
31. J. Matsui, N. Nakano, Z.Lj. Petrović, T. Makabe, *Appl. Phys. Lett.* **78**, 883 (2001)
32. S. Samukava, personal communication, 2001
33. M.J. Goeckner, T.K. Bennett, S.A. Cohen, *Appl. Phys. Lett.* **71**, 980 (1997)
34. G.J.M. Hagelaar, G.M.W. Kroesen, M.H. Klein, *J. Appl. Phys.* **88**, 2240 (2000)
35. J.P. Boeuf, L. Garrigues, L.C. Pitchford, in *Electron Kinetics and Applications of Glow Discharges*, edited by U. Kortshagen, L.D. Tsendin (Plenum Press, published in cooperation with NATO Scientific Affairs Division, New York and London, 1998), no. 367 in NATO ASI Series, pp. 85–100
36. A.V. Phelps, Z.Lj. Petrović, *Plasma Sources Sci. Technol.* **8**, R21 (1999)
37. A.V. Phelps, Z.Lj. Petrović, B.M. Jelenković, *Phys. Rev. E* **47**, 2852 (1993)
38. P. Hartmann, Z. Donkó, G. Bano, L. Szalai, K. Rózsa, *Plasma Sources Sci. Technol.* **9**, 183 (2000)
39. Z.Lj. Petrović, A.V. Phelps, *Phys. Rev. E* **56**, 5920 (1997)
40. S. Živanov, J. Živković, I. Stefanović, S.B. Vrhovac, Z.Lj. Petrović, *Eur. Phys. J. AP* **11**, 59 (2000)
41. A. Bogaerts, R. Gijbels, W.J. Goedheer, *J. Appl. Phys.* **78**, 2233 (1995)
42. Z. Donkó, *J. Appl. Phys.* **88**, 2226 (2000)
43. A.V. Phelps, L.C. Pitchford, C. Pedoussat, Z. Donkó, *Plasma Sources Sci. Technol.* **8**, B1 (1999)
44. A. Bogaerts, Z. Donkó, K. Kutasi, G. Bano, N. Pinhao, M. Pinheiro, *Spectrochim. Acta B* **55**, 1465 (2000)
45. Z.Lj. Petrović, V. Stojanović, *J. Vac. Sci. Technol. A* **16**, 329 (1998)
46. A.V. Phelps, B.M. Jelenković, *Phys. Rev. A* **38**, 2975 (1988)
47. D.A. Scott, A.V. Phelps, *Phys. Rev. A* **43**, 3043 (1991)
48. S.B. Vrhovac, B.M. Jelenković, J. Olthoff, R.V. Brunt, in *10th International Conference on Gas Discharges and their Applications*, edited by W.T. Williams, Department of Physics, University College of Swansea, Swansea, Wales, UK, 1992, p. 510
49. K. Kumar, H.R. Skullerud, R.E. Robson, *Aust. J. Phys.* **33**, 343 (1980)
50. G.H. Wannier, *Bell Syst. Tech. J.* **32**, 170 (1953)
51. H.R. Skullerud, *J. Phys. B: At. Mol. Phys.* **6**, 728 (1973)
52. R.E. Robson, *J. Phys. B: At. Mol. Phys.* **9**, L337 (1976)
53. T. Stefansson, H.R. Skullerud, *J. Phys. B: At. Mol. Opt. Phys.* **32**, 1057 (1999)
54. R. Hegerberg, M.T. Elford, H.R. Skullerud, *J. Phys. B: At. Mol. Phys.* **15**, 797 (1982)
55. H.W. Ellis, R.Y. Pai, E.W. McDaniel, E.A. Mason, L.A. Viehland, *At. Data Nucl. Data Tab.* **17**, 177 (1976)
56. G.N. Haddad, S.L. Lin, R.E. Robson, *Aust. J. Phys.* **34**, 243 (1981)
57. G. Sejkora, P. Girstmair, H.C. Bryant, T.D. Mark, *Phys. Rev. A* **29**, 3379 (1984)
58. B. Schiestl, W. Sejkora, M. Lezius, M. Foltin, T.D. Mark, in *8th Int. Seminar on Electron and Ion Swarm*, Abstracts of Papers, University of Trondheim, Norwegian Institute of Technology, Trondheim Norway, 1993, p. 65
59. H. Helm, M.T. Elford, *J. Phys. B: At. Mol. Phys.* **11**, 3939 (1978)
60. H.R. Skullerud, P.-H. Larsen, *J. Phys. B: At. Mol. Opt. Phys.* **23**, 1017 (1990)
61. E. Basurto, J. de Urquijo, I. Alvarez, C. Cisneros, *Phys. Rev. E* **61**, 3053 (2000)
62. T. Stefansson, *J. Phys. B: At. Mol. Opt. Phys.* **22**, 3541 (1989)
63. A.V. Phelps, unpublished, 1992
64. J.D. Urquijo, E. Basturto, A.V. Phelps, D. Piscitelli, L.C. Pitchford, *Bull. Am. Phys. Soc.* **45**, 47 (2000)
65. A. Hennad, O. Eichwald, M. Yousfi, O. Lamrous, *J. Phys. III France* **7**, 1877 (1997)